FINAL
IN-34-CR
0 AT.

67500

P.7

Final Report

Computation of Rotor–Stator Interaction Using the Navier–Stokes Equations

for
Dr. Eric McFarland
Grant Monitor

NASA Lewis Research Center
Grant NAG 3-869

by

David L. Whitfield
and
Jen-Ping Chen

CFD Lab

NSF Engineering Research Center for Computational Field Simulation

August 9, 1995

Mississippi State University
P.O. Box 6176
Mississippi State, MS 39762

Jen Ping Chen and David L. Whitfield,
CFD Lab., NSF Engineering Research Center
Mississippi State University

Numerical Scheme

This numerical scheme belongs to a family of codes known as UNCLE (UNsteady Computation of fieLd Equations) as reported by Whitfield (1995), that is being used to solve problems in a variety of areas including compressible and incompressible flows. This derivation is specifically developed for general unsteady multi–blade–row turbomachinery problems.

The scheme solves the Reynolds–averaged N–S equations with the Baldwin–Lomax turbulence model. In Chen's work (1993), the governing equations are cast in time–dependent curvilinear coordinates with conservative variables written in inertial Cartesian coordinates,

$$\frac{\partial Q}{\partial \tau} + \frac{\partial F}{\partial \xi} + \frac{\partial G}{\partial \eta} + \frac{\partial H}{\partial \zeta} = \frac{\partial G^d}{\partial \eta} + \frac{\partial H^d}{\partial \zeta} \qquad (1)$$

Q is the conservative variable vector, F, G, H are the convective flux vectors in the curvilinear directions ξ, η, ζ respectively. G^d and H^d are the viscous flux vectors. A finite volume discretization is applied to the above, and a general implicit scheme is used to integrate the discretized equation in time with second order accuracy as explained in Janus (1990).

The resulting numerical expression can be symbolically written as a nonlinear system

$$S\,(\,Q^{n+1}\,) = 0 \qquad (2)$$

where n+1 denotes the new time step. The convective flux in Eq. (2) is evaluated by Roe's flux–difference–splitting which is first order accurate in space. High order accuracy of the flux is obtained through the use of limiters. The viscous flux is central–differenced and is second order accurate.

For a flow which is steady in time Q^{n+1} will converge to a value which is independent of n. If one is not interested in the transient state, all that matters is the value of Q^{n+1} as n becomes larger. However for a time dependent flow, the intermediate values of Q^{n+1} are of importance for they represent the state of the fluid at time n+1. For unsteady flows, Equation (2) must be solved to within truncation error at each instant in time. The UNCLE code uses the Newton procedure,

$$S'(Q^{n+1,k})\,(Q^{n+1,k+1} - Q^{n+1,k}) = S\,(Q^{n+1,k}) \tag{3}$$

to solve Eq. (2). The variable k is the Newton iteration count and $S'(Q^{n+1,k})$ is the Jacobian matrix. The inviscid contributions to S' are based on a flux–vector splitting technique. Following the work of Taylor (1992), the viscous contributions are evaluated numerically. The inversion of Eq. (3) at any k is by means of a symmetrical Gauss–Seidel iteration procedure.

Boundary Conditions

The inlet boundary is specified by a characteristic–based one–dimensional boundary condition in an attempt to preserve the specified radial distribution of total temperature and total pressure. The exit boundary is also specified by a characteristic type boundary condition making use of the radial momentum equilibrium that accounts for swirl produced downstream of the rotating blades. Adiabatic–wall and no–slip conditions are employed at impermeable surfaces. For boundaries at the interface of adjacent blade passages, the periodic boundary condition is used.

Tip Treatment

Tip clearance is modeled by assuming the gap region is periodic. This means the flow is transported tangentially without a loss of mass, momentum and energy. The effect of vena contracta is considered by reducing the size of the real tip clearance to half. Detail of this model can be found in Kirtley at al. (1990). The present tip treatment is not exact because the tip model leads to a simplified grid that has a void inside the tip region. It is the authors' feeling that the correct tip treatment could be important to resolve the wake close to the casing. An effort of computing instead of modeling the tip region by adding another grid block inside the tip region is underway.

Turbulence Model

The turbulence model used in this work is the Baldwin–Lomax model. A wall function approximation has been incorporated into the code which allows the center of the first grid cell off the wall to be positioned much further out in the flow, hence reducing the total number of grid points.

Results and Discussions

An H–grid of 132 points streamwise, 51 points spanwise and 41 points pitchwise was used. The original computed pressure ratio vs. mass flow is shown in Fig. 1. These numerical results were obtained by time averaging the time accurate simulations, the time step being 1/40th of the blade passing cycle. As a result, each operating point of Fig.1 requires 10.4 CPU hours on Cray C90.

With the exception of the pressure ratio and efficiency vs. mass flow plots, all of the remaining results that were presented at the ASME blind test case session are for an arbitrary instant in time. Subsequently, it was found that the results were time dependent. It appears in further examination of the flow field at the maximum flow condition that both the near hub and tip regions are the sources of the unsteady behavior. The time average spanwise total pressure ratio distribution at station 4 (postdiction) is shown in Fig. 2 along with the predicted results at an arbitrary instant in time. The time average results appear to be in better agreement with the measurements near the hub region than the predicted results. The postdicted result of Fig. 2 is the time average over a cycle of rotor revolution. Further study is needed to assess the cause of the unsteady behavior.

ACKNOWLEDGEMENTS

Special thanks go to Dr. John Adamczyk for his kind help in interpreting the computed flow field.

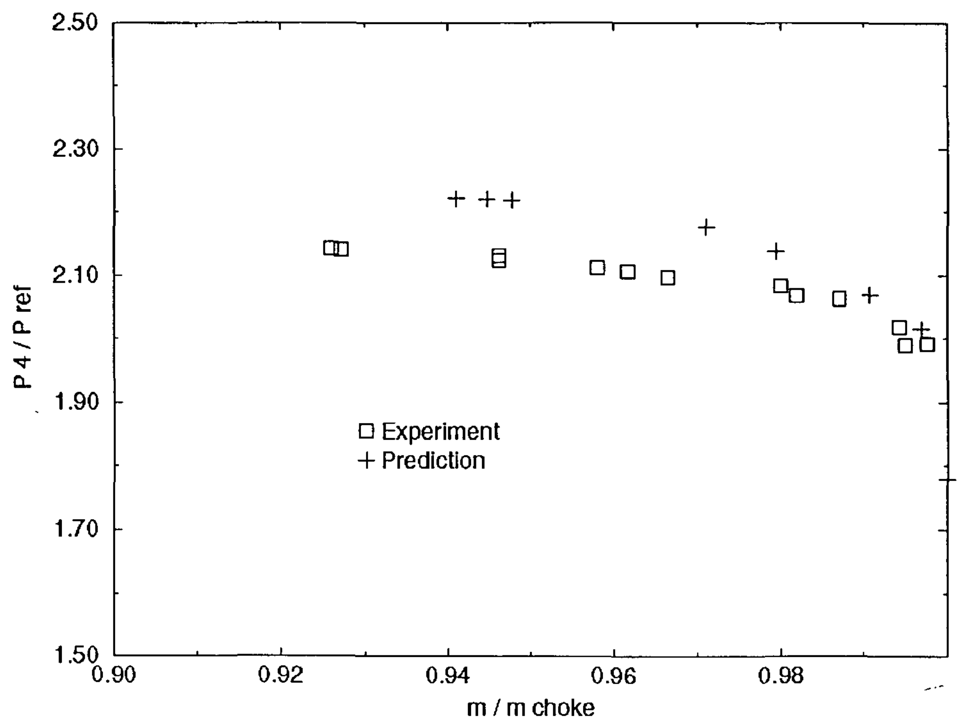

Figure 1 Pressure Ratio vs. Mass Flow

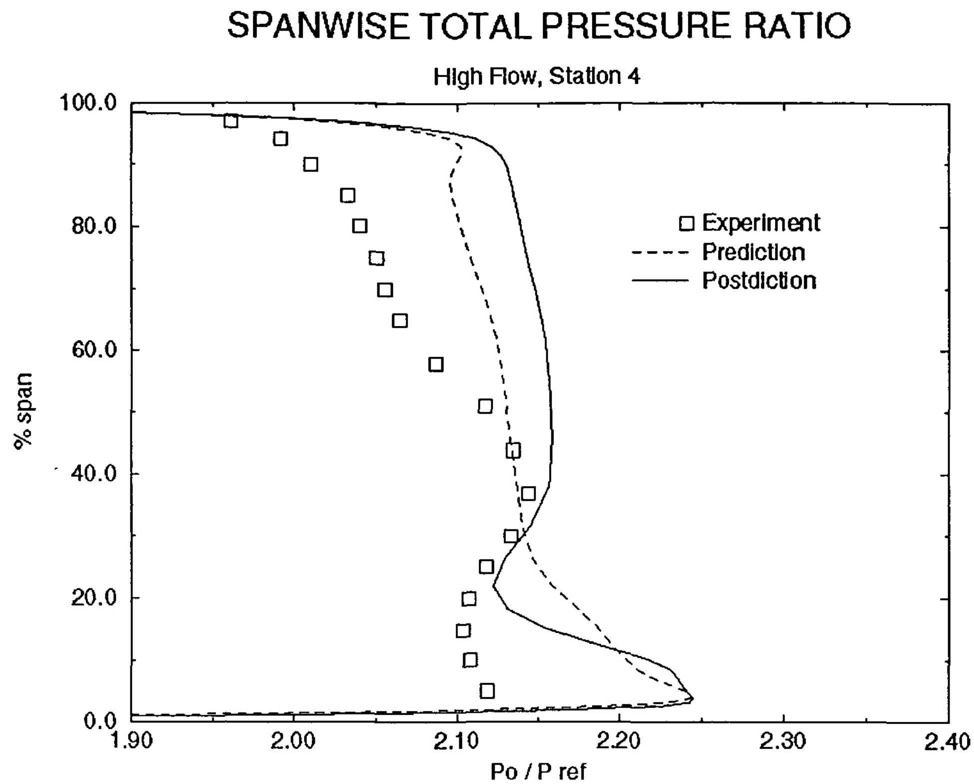

Figure 2 Spanwise Distribution of Total Pressure Ratio at Station 4, High Flow.

References

Chen, J.P. and Whitfield, D.L., 1993, "Navier–Stokes Calculations for the Unsteady Flowfield of Turbomachinery," *AIAA–93–0676*.

Janus, J.M., and Whitfield, D.L., 1990, "Counterrotating Prop–Fan Simulations Which Feature a Relative–Motion Multiblock Grid Decomposition Enabling Arbitrary Time–Steps," *AIAA–90–0687*.

Kirtley, K.R., Beach, T.A., and Adamczyk, J.J., 1990, "Numerical Analysis of Secondary Flow in a Two–Stage Turbine," *AIAA–90–2356*.

Taylor, L.K., Busby, J.A., Jiang, M.Y., Arabshahi, A., Sreenivas, K., and Whitfield, D.L., 1993, "Time Accurate Incompressible Navier–Stokes Simulation of the Flapping Foil Experiment," Sixth International Con. on Numerical Ship Hydrodynamics.

Whitfield, D.L., 1995, "Perspective on Applied CFD," AIAA–95–0349.